Full Paper

Journal of the Brazilian Chemical Society

https://dx.doi.org/10.21577/0103-5053.20260085

J. Braz. Chem. Soc. **2026**, *37*, e-20260085, 1-18

Deep Eutectic Solvents as Green Catalysts for Carbohydrate Conversion and Synthesis of Furanic Compounds from Amazonian Cupuaçu Peel (*Theobroma grandiflorum*)

Douglas M. da Costa, [a] ***Jéssyka R. Santos,*** [b] ***Amanda A. Rodrigues,*** [c] ***Joênes M. Peluzio,*** [a] ***Daniel A. Bertuol,*** [d] ***Gustavo G. Pinto,*** [e] ***Clarissa P. Frizzo*** [e] ***and Elisandra Scapin*** *[a,b,c]

[a]*Programa de Pós-Graduação em Biodiversidade e Biotecnologia, Universidade Federal do Tocantins, 77001-090 Palmas-TO, Brazil*

[b]*Programa de Pós-Graduação em Ciências Ambientais, Universidade Federal do Tocantins, 77001-090 Palmas-TO, Brazil*

[c]*Curso de Engenharia Ambiental, Universidade Federal do Tocantins, 77001-090 Palmas-TO, Brazil*

[d]*Laboratório de Processos Ambientais, Universidade Federal de Santa Maria, 97105-900 Santa Maria-RS, Brazil*

[e]*Departamento de Química, Universidade Federal de Santa Maria, 97105-900 Santa Maria-RS, Brazil*

Lignocellulosic biomass is a promising renewable feedstock, but its high recalcitrance requires biotechnological pretreatments to enable conversion into biobased chemicals. This study evaluated deep eutectic solvent (DES) pretreatments to maximize carbohydrate conversion and optimize the production of furanics 5-hydroxymethylfurfural (HMF) and furfural (FF) from cupuaçu peel (CP). Pretreatment was performed with choline chloride (ChCl)-based DES combined with lactic acid (LA), oxalic acid (OA) or ethylene glycol (EG), using ultrasound (US) or autoclave (ATC). Pretreatments with DES proved effective in structurally modifying biomass, as evidenced by Fourier transform infrared (FTIR), X-ray diffraction (XRD), scanning electron microscopy (SEM) and thermogravimetric analyses (TGA). After acid hydrolysis, ChCl:OA + ATC and ChCl:OA + US increased glucose concentrations by 97.90 and 69.72%, respectively, relative to raw CP. Analysis of variance (ANOVA) revealed a significant interaction between DES type and pretreatment method ($p < 0.05$). The synthesis of HMF and FF from cupuaçu peel hydrolysate was optimized in a DES/ethyl acetate system, achieving yields of 1.46 and 7.80%, respectively, at 120 °C for 150 min. The results show that the integration of DES combined with US and ATC technologies represents a sustainable and promising strategy for the valorization of Amazonian lignocellulosic waste in the context of biorefineries.

Keywords: DES, lignocellulosic biomass, furanic compounds, green chemistry

Introduction

The growing demand for clean and renewable energy sources is a key factor in addressing the environmental and climate crisis. In this context, lignocellulosic biomass emerges as a major alternative in the energy transition, representing a promising option for the production of bioproducts in biorefineries, while reconciling the environmental, economic, and social dimensions of sustainability.[1] Among lignocellulosic biomasses, agricultural byproducts and residues from the food and paper industries, among others, are particularly noteworthy.[2]

Plant-derived residues constitute the most abundant source of unused or underutilized biomass worldwide. This renewable resource has attracted growing interest for the production of molecules aimed at the manufacture of biofuels, functional materials, and bio-based chemicals.[3,4] However, the processing of lignocellulosic biomass is hindered by its low solubility in water and in various

*e-mail: scapin@mail.uft.edu.br
Editor handled this article: João H. G. Lago (Associate)

organic solvents, a feature attributed to its complex fibrous structure.[5] Its composition consists predominantly of polysaccharides, such as cellulose and hemicellulose, linked by a lignin matrix, which imparts high resistance and structural complexity. This recalcitrance hinders access to cellulose, acting as a protective barrier and making the process even more challenging.[6,7]

For lignocellulosic materials, pretreatment promotes the cleavage of chemical bonds that connect the subunits or oligomeric units of structural polymers, resulting in the deconstruction of the lignocellulosic matrix and facilitating the penetration of reagents.[5] Currently, there is a wide variety of pretreatment methods, applied either individually or in combination, that promote the disruption of the microstructure of lignocellulosic biomass, reducing cellulose crystallinity, increasing porosity, and favoring lignin removal.[8]

Among the technological alternatives for the valorization of lignocellulosic biomass, deep eutectic solvents (DES) have emerged as a promising, low-cost route with strong environmental appeal, since they are formed by the interaction between a hydrogen bond donor and a hydrogen bond acceptor.[9] These solvents show high efficiency in the removal of lignin and hemicellulose during pretreatment, increasing cellulose accessibility and favoring its conversion into fermentable sugars.[10]

In this context, DES have received growing attention as a pretreatment strategy in sustainable biorefineries because they feature a short production cycle, low cost, renewable character, and high environmental compatibility.[11] The use of DES is further highlighted by their high biomass solubilization capacity, easy synthesis, low volatility, non-flammable nature, biodegradability, and reduced toxicity, making them a promising alternative for the pretreatment of lignocellulosic biomass.[12]

Biorefineries play a central role in the conversion of lignocellulosic biomass into high value-added products, among which 5-hydroxymethylfurfural (HMF) and furfural (FF) stand out. These compounds, regarded as platform chemicals, are essential organic molecules that can be readily obtained and are widely employed in various industrial applications.[13,14]

Brazil has great potential to be explored, especially in the Legal Amazon region, which harbors vast plant biodiversity. Among its most notable resources are high-yield fruit species that generate residues rich in lignocellulosic biomass.[15] The cupuaçu tree *Theobroma grandiflorum* (Willd. ex Spreng.) Schum, belonging to the Malvaceae family, is a fruit species native to the Southern region of the Amazon River and the Western region of the Tapajós River, and is widely distributed across the states of the Northern region, as well as the south and Southeast of Pará and the pre-Amazon region of Maranhão.[16]

Cupuaçu peel is the main residue generated from the fruit, accounting for approximately 45% of its total weight.[17] This byproduct, which has been increasingly valued, represents a promising source of lignocellulosic biomass for the synthesis of biocompounds through processes such as acid hydrolysis and pyrolysis.[18,19] Cupuaçu husk biomass has high levels of glucan (56.49%) and xylan (15.66%), low extractives content (5.89%), and limited current use, indicating an advantage over sugarcane biomass, which is already widely used.[20] Advances and prospects in the integral utilization of residues in biorefineries reinforce the role of lignocellulosic biomass as a strategic source both for energy generation and for the synthesis of biocompounds, contributing to the diversification of cleaner and more sustainable energy matrices.

Therefore, the present study aims to evaluate deep eutectic solvent (DES)-based pretreatment routes for cupuaçu peel, focusing on increasing carbohydrate release and optimizing the synthesis of the furanic compounds HMF and FF, with DES being employed in both the pretreatment and furanic-synthesis steps. The valorization of plant biomass, combined with the use of green solvents, represents an innovative and sustainable strategy for the efficient conversion of lignocellulosic residues into high value-added bioproducts.

Experimental

Figure 1 schematically illustrates the development of the study, starting with the physical treatment of cupuaçu peel, proceeding through different pretreatment methodologies, and ultimately resulting in the optimization of furanic compounds.

Samples

Cupuaçu fruits (*Theobroma grandiflorum*) were purchased from local markets of the farmers in the city of Palmas-TO, Brazil. The cupuaçu peels were washed, broken into smaller pieces, and dried in a forced-air oven at 65 °C for 48 h. The dehydrated peels were ground in a Willey-type knife mill (Start FT 50, Fortinox) and sieved (24 mesh) to obtain particles smaller than 710 μm. The processed material was then stored in airtight glass bottles for later use.

Proximate analysis

The procedures used for proximate analysis were carried out in accordance with the standards of the

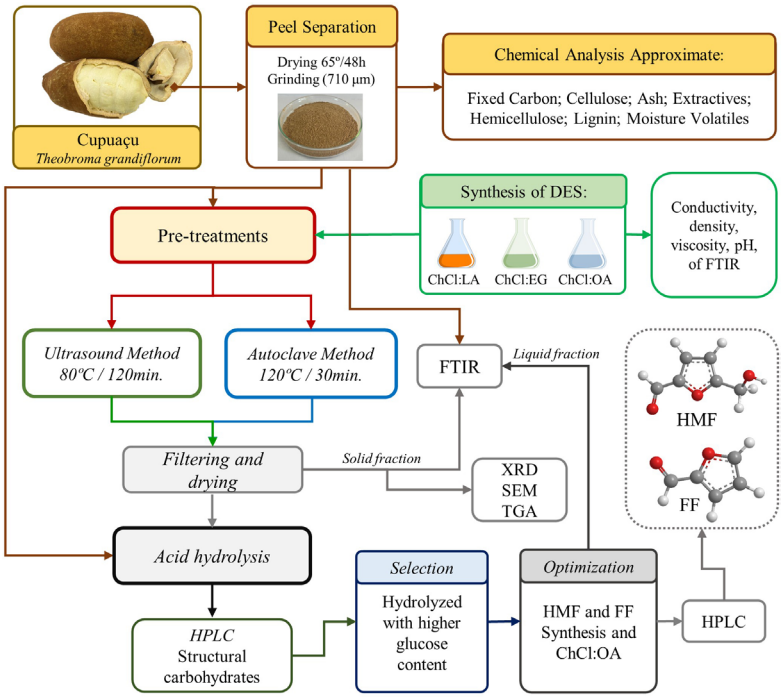

Figure 1. Flowchart of the process from pretreatment to the synthesis of HMF and FF.

American Society for Testing and Materials (ASTM). The four components analyzed were: moisture (ASTM D3173-03);[21] volatile matter (ASTM D3175-07);[22] ash content (ASTM D3174-04);[23] and fixed carbon, calculated as the difference between 100 and the sum of the percentages of moisture, volatile matter, and ash.

Extractives

Extractives analysis was carried out in a Soxhlet extractor (MA 044/08/50) using approximately 3 g of raw sample and 190 mL of ethanol (95%) under reflux for 8 h, following the methodology of the National Renewable Energy Laboratory (NREL).[24] After completion of the reflux, the thimbles were removed and placed on Petri dishes on the bench for 48 h to dry. The initial and final masses of the samples were measured, and the extractives content (%) was determined using equation 1:

$$\text{Extractives} = \frac{\text{mass of extract}}{\text{mass of raw sample}} \times 100 \quad (1)$$

Cellulose and hemicellulose content

Neutral detergent fiber (NDF) was determined according to method INCT-CA F-002/1, and acid detergent fiber (ADF) according to method INCT-CA F-004/1.[25] The fibrous component of the biomass (hemicellulose) was determined as the difference between the NDF and ADF contents.[26] The cellulose fraction was obtained by difference between the hemicellulose and lignin contents, as described by Ding *et al.*,[27] and is represented in equation 2:

$$\text{Cellulose} = \text{NDF} - (\text{hemicellulose} + \text{ligning}) \quad (2)$$

Lignin content

The insoluble lignin content was determined according to the Klason method as modified by Rocha.[28] After acid hydrolysis, the samples were filtered and the residue retained on the filter paper was washed with 1500 mL of distilled water, transferred to weighing dishes, and dried in an oven at 100 °C to constant mass. The percentage of insoluble lignin (L_{ki}) was calculated relative to the dry sample mass, as shown in equation 3:

$$L_{ki} = \frac{M_k - M_c}{M_a} \times 100 \quad (3)$$

where, M_k: mass of dry insoluble lignin, M_c: mass of ash, M_a: dry mass of the sample used in the analysis.

Synthesis of deep eutectic solvents (DES)

The DES used in this study were synthesized by combining the hydrogen bond acceptor (HBA), choline chloride (ChCl), with different hydrogen bond donors (HBD): lactic acid, ethylene glycol, and oxalic

acid. The mixtures were prepared at molar ratios of 1:2 (ChCl:lactic acid), 1:1 (ChCl:ethylene glycol), and 1:1 (ChCl:oxalic acid) (Figure 2). The synthesis was carried out in a water bath at 90 °C under constant stirring until a homogeneous liquid (with no solid residues in suspension) was obtained, according to Zhang *et al.*,[29] with adaptations.

After synthesis, the DES were hermetically sealed, cooled to room temperature, and stored in a desiccator. Conductivity, density, viscosity, and pH were measured at 25 ºC, and Fourier transform infrared (FTIR) spectra were recorded using a CARY 630 spectrometer. The apparent pH of the DES used in the study was determined after dilution to 30% (v/v) in ultrapure water, using a Hanna® pH meter model HI5221.

Pretreatments with DES

For the pretreatments, 2 g of cupuaçu peel were treated with different DES (ChCl:LA, ChCl:EG, and ChCl:OA) using two distinct methodologies: ultrasound (US) and autoclave (ATC). The suspensions were prepared at a solid-to-liquid ratio of 1:10 (g mL^{-1}, m/v), with the addition of 30% (v/v) H_2O to control viscosity, and subjected to shaking in a shaker at 60 °C for 10 min to ensure homogenization.[30] The US methodology was carried out according to Pradhan *et al.*,[31] with modifications, using an ultrasonic bath operating at 25 kHz (Q 5.9/25A, Ultronique) at 80 °C for 120 min. For the ATC methodology, performed according to Huang *et al.*,[32] with modifications, the samples were autoclaved at 120 °C for 30 min. In the subsequent step, the samples were filtered through filter paper and washed with distilled water to completely remove the DES used in the pretreatment. The insoluble residue obtained after filtration was dried in a forced-air oven at 60 °C for 24 h and subsequently collected for acid hydrolysis.

Acid hydrolysis

Acid hydrolysis of raw biomass and of the samples pretreated with different DES using ultrasound and autoclave methods was performed according to the methodology described by Dunning and Dallas.[33] Two grams of sample were used, to which 10 mL of 72% sulfuric acid (H_2SO_4) were added, followed by heating and stirring at 50 °C for 7 min. Subsequently, 40 mL of distilled water were added, and the mixture was autoclaved at 121 °C for 15 min. The resulting material was filtered and stored for further analyses.

Fourier transform infrared (FTIR) spectroscopy

The DES, raw biomass, and the solid fraction after pretreatment were analyzed using a CARY 630 FTIR spectrometer (Agilent technologies). The analyses covered the range from 4,000 to 650 cm^{-1}, with a resolution of 4 cm^{-1} and 32 scans *per* spectrum.

X-ray diffraction (XRD) analysis

The crystallinity of the raw biomass and of the solid fraction after acid hydrolysis of the pretreated samples was measured using an X-ray diffractometer (XRD) (Bruker D8 Advance, Karlsruhe, Germany). The samples were previously dried at 80 °C. The scan was carried out over the 2θ range from 5° to 35° using Cu Kα radiation, with a step size of 0.05° and a counting time of 10 s. The crystallinity index was calculated according to Sasmal *et al.*,[34] using the intensity method, based on equation 4:

$$CrI = \frac{Ic - Ia}{Ic} \times 100 \quad (4)$$

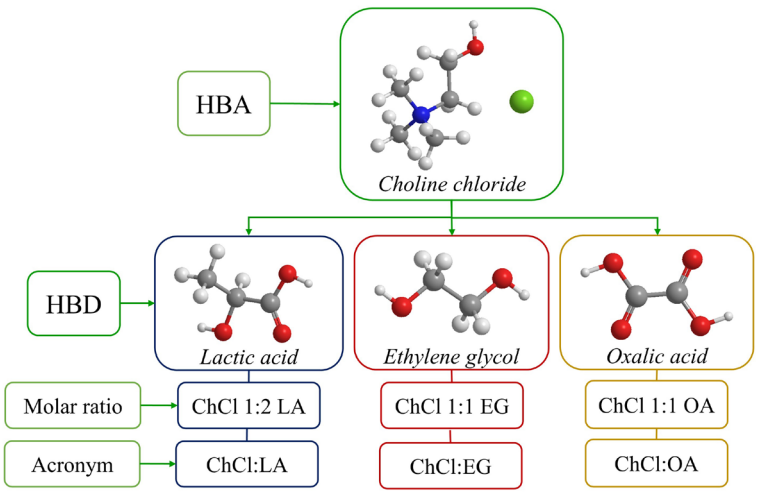

Figure 2. Composition of the DES used in the study.

where, CrI (%): crystallinity index, Ic: intensity at 22-23°, Ia: intensity at 18-19°.

Scanning electron microscopy (SEM)

High-resolution images were obtained using a scanning electron microscope (Shimadzu SSX-550, Kyoto, Japan). The samples were dried at 60 °C and coated with an Au/Pd film. Images were acquired at magnifications ranging from 300 to 5000×, using an accelerating voltage of 10 kV.

Thermogravimetric analysis (TGA)

The thermogravimetric analysis (TGA) experiments were performed using a TGA Q5000 instrument (TA Instruments Inc., USA). The equipment usage condition was accessed by measuring the mass loss of a sample of well-known thermal decomposition profile ($CaC_2O_4.H_2O$ 99.9%). Thermal characterization analyses were carried out at a heating rate of 10 °C min^{-1} up to 900 °C. The sample mass used was approximately 7 mg. An inert nitrogen (N_2) atmosphere was employed at a flow rate of 25 mL min^{-1}. The sample was not dried before analysis, and no isothermal treatment was performed to remove possible volatile interferents (residual solvents and/or water). Data was processed using TA Universal Analysis 2000 software, version 4.5 (TA Instruments Inc., USA), and OriginPro 9.5 (Northampton, MA, USA).

Statistical analysis of pretreatment data

For the variables glucose yield (g L^{-1}) and xylose yield (g L^{-1}), the experiment was conducted in a completely randomized design with three replicates at the central point, following a 2 × 3 + 1 factorial arrangement. The design consisted of two methods (ultrasound and autoclave), three types of DES (ChCl:LA, ChCl:EG, and ChCl:OA), and one additional treatment (raw cupuaçu peel). Analysis of variance (ANOVA) was performed at $\alpha = 0.05$, and the factor means were subsequently compared using the Scott-Knott test at the 5% significance level ($\alpha = 0.05$), with the aid of the AgroEstat 7.0 software.[35]

The mean of the additional treatment was compared with the factor means using the test of Dunnett at the 5% significance level ($\alpha = 0.05$), with the aid of the GENES 5.1 software (Universidade Federal de Viçosa, Brazil, 2013).[36]

Synthesis of the furanic compounds HMF and FF

After quantification of the carbohydrates in the samples pretreated with DES, the hydrolysate from the ChCl:OA + ATC system, which showed the highest glucose yield, was selected for the synthesis of HMF and FF. In a 50 mL round-bottom flask, 2.5 mL of hydrolysate, 2.5 mL of the ChCl:OA DES, and 2.5 mL of ethyl acetate were added.[37,38] The reaction was carried out in an oil bath under constant stirring, at temperatures ranging from 100 to 140 °C and reaction times between 90 and 150 min, according to the experimental design (Table 1), kept under reflux. After completion of the reaction time, the samples were washed three times with ethyl acetate, followed by the addition of anhydrous sodium sulfate and filtration. The resulting product was subjected to HMF and FF quantification.

Experimental design

The experimental design and analysis of HMF and FF synthesis were carried out using the Protimiza experimental design software,[39] based on the studies conducted by Scapin *et al.*,[38] varying temperature and reaction time (Table 1). A face-centered design (FCD) was used with a 2^2 factorial arrangement, with 4 trials on the face-centered surfaces and 3 repetitions at the central point, totaling 11 experimental trials.

High-performance liquid chromatography (HPLC) analysis

Monomeric sugars in the raw and pretreated samples were quantified by high-performance liquid chromatography (HPLC) using a Shimadzu chromatograph (LC-10A series, Kyoto, Japan). Glucose and xylose were determined using a Phenomenex Rezex ROA-organic acid H^+ (8%) column and 0.005 mol L^{-1} H_2SO_4 as the eluent, with a flow rate of 0.4 mL min^{-1} and a column temperature of 60 °C. A refractive index detector (SPD-10A VP, Shimadzu) was used. The compound yields were calculated from calibration curves obtained from standard solutions ($R^2 > 99\%$).

HMF and FF contents were evaluated by HPLC using a Shimadzu chromatograph (LC-6AD series) equipped with a refractive index detector (RID-10A) and an ultraviolet-visible (UV-Vis) diode array detector (DAD) set at a wavelength of 276 nm. A supelcogel C-610H column (30 cm × 7.7 mm) was used at 55 °C, with 0.0005 mol L^{-1} H_2SO_4 as the mobile phase at a flow rate of 0.6 mL min^{-1}. The concentrations of the analyzed compounds were determined from analytical calibration curves prepared with standards, with coefficients of determination $R^2 > 99\%$ for both HMF and FF. The yields (%) of the furanic compounds HMF and FF were calculated using equations 5 and 6, as proposed by Cai *et al.*:[40]

Table 1. Face-centered design (FCD) matrix for optimization of HMF and FF synthesis yields using hydrolysate from cupuaçu peel pretreated with ChCl:OA, combined with an autoclave

Assay	Temperature / ºC	time / min	HMF		FF	
			Concentration / (mg L^{-1})	Yield / %	Concentration / (mg L^{-1})	Yield / %
1	100	90	127.83	0.90	111.00	4.24
2	140	90	111.36	0.78	92.84	3.55
3	100	150	130.27	0.92	138.68	5.30
4	140	150	182.52	1.28	150.50	5.75
5	100	120	117.04	0.82	115.08	4.40
6	140	120	197.47	1.39	170.51	6.51
7	120	90	153.63	1.08	132.29	5.05
8	120	150	207.31	1.46	204.14	7.80
9	120	120	165.81	1.17	152.64	5.83
10	120	120	170.85	1.20	145.90	5.57
11	120	120	153.82	1.08	136.51	5.21

HMF: 5-hydroxymethylfurfural; FF: furfural.

$$\text{Yield}_{HMF} = \frac{\left(\left(C_{HMF} \times V_h\right)/126\right)}{\left(m_{cell}/162\right)} \times 100 \quad (5)$$

$$\text{Yield}_{FF} = \frac{\left(\left(C_{FF} \times V_h\right)/96\right)}{\left(m_{hem}/132\right)} \times 100 \quad (6)$$

where, C_{HMF}: HMF concentration (mg L^{-1}), C_{FF}: FF concentration (mg L^{-1}), V_h: hydrolysate volume (0.0025 L), m_{cell}: cellulose mass (mg), m_{hem}: hemicellulose mass (mg).

Results and Discussion

Determination of biomass chemical composition

Table 2 shows the chemical composition of raw cupuaçu peel. The chemical characterization of cupuaçu peel showed that this biomass is a promising feedstock in biorefineries, mainly due to its high content of structural carbohydrates, such as cellulose and hemicellulose, which together account for 54.68%. This value was higher than that reported by Suárez-Patlán *et al.*,[41] who found 49.5% when analyzing cocoa pod husk using a similar methodology. However, the high lignin content (about 32.3%) may pose a challenge for pretreatment processes.

Table 2. Chemical composition of raw cupuaçu peel

Component	Content / %
Fixed carbon	7.51 ± 0.15
Cellulose	45.68 ± 1.50
Ash	2.18 ± 0.15
Extractives	3.61 ± 0.34
Hemicellulose	9.00 ± 1.49
Lignin	32.30 ± 0.33
Moisture	4.89 ± 0.10
Volatiles	85.42 ± 0.85

The low moisture (4.89%) and ash (2.18%) contents found in this study differ from the values reported by Silva *et al.*,[42] who observed 11.00% moisture and 1.99% ash. Lower values for these parameters are favorable, as they are directly associated with higher bioproduct yields and greater efficiency of acid hydrolysis.[43]

The fixed carbon content determined was 7.51%, a value similar to that reported by Estacio and Hoyos,[44] who obtained 7.49% when studying cocoa almond husk. Finally, the volatile matter content obtained was 85.42%, similar value to those reported by Borges *et al.*,[18] who identified 79.73% for cupuaçu peel and 84.81% for baru husk. The high volatile matter content of cupuaçu peel correlates with the quality of the lignocellulosic biomass, allowing efficient combustion at lower temperatures and increasing the immediate availability of energy.[45]

Physicochemical characterization of DES

Table 3 shows the physicochemical characterization (conductivity, density, viscosity, and pH apparent) of the DES used in this work. The results are in agreement with data reported in the literature.[46,47]

The ChCl:OA DES showed the highest values of conductivity (414.3 mS m^{-1}), density (1.225 g cm^{-3}), and viscosity (166.55 cP), as well as the lowest pH value (–0.61). Parameters such as conductivity and pH modulate intermolecular interactions, favoring the diffusion of reagents and, consequently, increasing the efficiency of biomass pretreatment.[48] However, the high viscosity of

Table 3. Physicochemical characterization of DES

Type	Conductivity / (mS m^{-1})	Density / (g cm^{-3})	Viscosity / cP	pH
ChCl 1:2 LA	346.0 ± 1.10	1.161 ± 0.07	108.88 ± 1.85	0.56 ± 0.02
ChCl 1:1 EG	50.5 ± 1.56	1.114 ± 0.05	60.06 ± 1.25	5.04 ± 0.06
ChCl 1:1 OA	414.3 ± 1.43	1.225 ± 0.02	166.55 ± 1.20	–0.61 ± 0.01

ChCl: choline chloride; LA: lactic acid; EG: ethylene glycol; OA: oxalic acid.

deep eutectic solvents (DES) impairs ion mobility and hinders the interaction between the solvent and the biomass, making system dilution an essential factor for process performance.[29] It is worth noting that the viscosity of DES directly influences ionic mobility and, consequently, the transport properties of the system. High viscosity tends to restrict the translational movement of ionic species, reducing their mobility and, therefore, the ionic conductivity of the medium. Thus, an inverse relationship is generally observed between viscosity and ionic mobility, in which less viscous systems exhibit greater charge transport capacity.[49] This relationship is essential to explain how the controlled addition of water reduces the viscosity of DES, promoting greater ionic mobility and improving the transport properties of the system.[50]

The ChCl:EG DES showed the lowest conductivity (50.5 mS m^{-1}) and viscosity (60.06 cP), as well as a pH close to neutrality (5.04). These results indicate milder interactions with the biomass, which may confer greater selectivity in disrupting lignocellulosic fractions and favor targeted extraction processes.[51] Finally, the ChCl:LA DES presented intermediate density (1.161 g cm^{-3}) and viscosity (108.88 cP) values, associated with a strongly acidic pH (0.56), a condition that may favor hydrolysis reactions.[52] Each DES exhibits specific properties that can directly affect pretreatment performance, resulting in different behaviors in the deconstruction of lignocellulosic biomass.

FTIR analysis

The synthesis of the DES was confirmed by Fourier transform infrared (FTIR) spectroscopy (Figure 3), based on the appearance of bands corresponding to the main functional groups and on data reported in the literature.[3,53]

In the DES of ChCl:LA and CHCl:OA, an intense peak was observed at 1719 cm^{-1}, attributed to the C=O stretching vibration of carboxylic groups present in lactic and oxalic acids, which act as HBD in the solvent composition (Figure 3). Sari *et al.*[47] reported that the presence of a band around 1719 cm^{-1} may be associated with a shift of carbonyl groups involved in hydrogen bonding, due to stabilization promoted by interactions with the HBA. According to

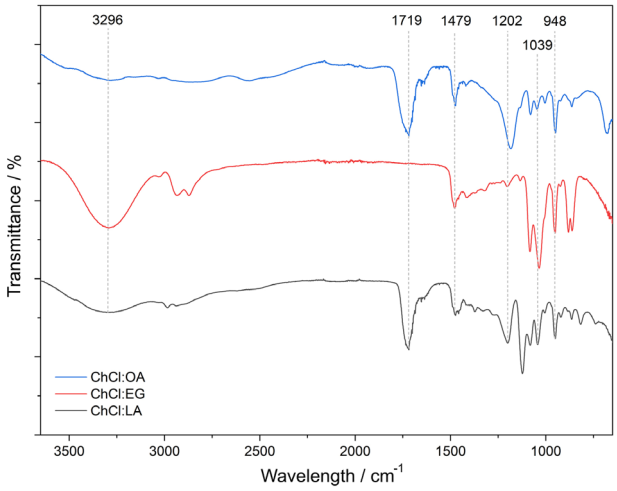

Figure 3. FTIR spectra of the DES used in the pretreatment.

Amesho *et al.*,[3] the presence of bands at 1039 and 948 cm^{-1} in DES FTIR spectra is associated, respectively, with C–O vibrations, and C–O–C stretching, all of which were observed in every DES.

The bands between 1400 and 1000 cm^{-1} can be attributed to C–O vibrations associated with interactions between choline chloride, which acts as the HBA, and the HBDs. These interactions are critical for the performance of DES.[54] In addition, in the ChCl:EG DES a characteristic band was observed at 3296 cm^{-1}, which may be related to O–H stretching vibrations, a fingerprint of hydroxyl groups present in alcohols such as ethylene glycol.[55]

The raw biomass and the solid fraction after pretreatment with different DES using distinct methods were also analyzed by FTIR (Figure 4).

After pretreatment, the band at 1027 cm^{-1} in the solids obtained from pretreated cupuaçu peel showed a reduction in intensity, which became more evident in the ChCl:OA + US system and in all methods that used autoclave, when compared with raw cupuaçu peel. According to Makarem *et al.*,[56] this band can be associated with C–O stretching in aryl-alkyl ether linkages, typical structural components of cellulose and hemicellulose in lignocellulosic biomass, suggesting that part of this fraction was degraded or converted into monomeric carbohydrates during DES pretreatments. This effect was particularly pronounced for all DES systems combined

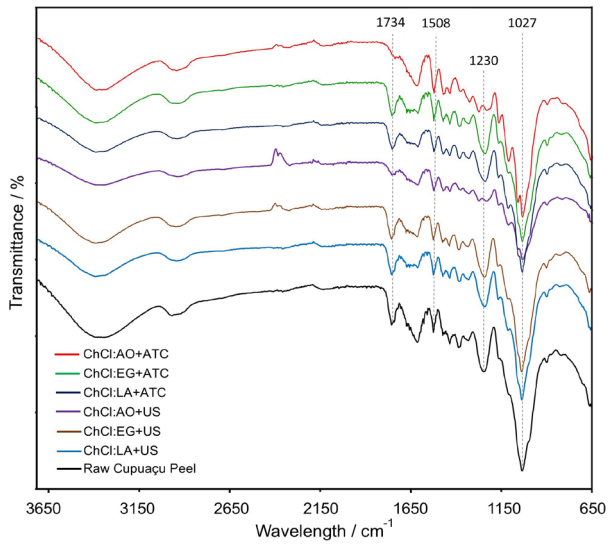

Figure 4. FTIR spectra of raw cupuaçu peel and of the solid fraction of samples after pretreatment with different DES combined with ultrasound (US) or autoclave (ATC).

with autoclave and for ChCl:OA when ultrasound was used.

Notable changes were observed in the band at 1230 cm^{-1}, related to C–O–C stretching vibrations of cellulose and hemicellulose. Narrowing of this band after pretreatment with ChCl:OA DES in both methods indicates that the processes favored exposure of the cellulosic fraction.[29]

According to Roslan *et al.*,[57] the peak at 1517 cm^{-1} can be attributed to skeletal vibrations of the aromatic ring in lignin. The band at 1739 cm^{-1} may be attributed to C=O stretching of ester groups present in acetylated hemicellulose.[58] A reduction in the intensity of this band was observed after pretreatments with ChCl:OA in both methods, indicating a differentiated structural modification of the lignocellulosic biomass promoted by this DES. Armed *et al.*[53] also associate the band around 1739 cm^{-1} with carbonyl C=O stretching vibrations in hemicellulose.

Figure 5 shows the FTIR spectra of hydrolysates from raw cupuaçu peel and peel pretreated with ChCl:OA DES, together with the organic phase from furan synthesis corresponding to assays 2 (140 °C for 90 min) and 8 (120 °C for 150 min) of the FCD optimization (Table 1).

The FTIR spectra of hydrolysates obtained from raw cupuaçu peel and from samples pretreated with ChCl:OA DES showed a broad band in the region of 3296 cm^{-1}, attributed to O–H stretching vibrations of hydroxyl groups.[59] During acid hydrolysis, partial cleavage of glycosidic bonds occurs, leading to the formation of oligosaccharides and monosaccharides with free –OH groups, which contributes to the broadening and increased intensity of this band.[60] In addition, a band was observed

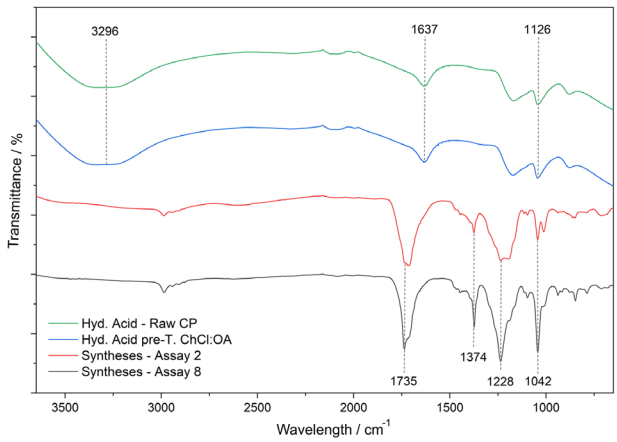

Figure 5. FTIR spectra of hydrolysates (Hyd.) from raw cupuaçu peel and peel pretreated with ChCl:OA, and of the organic fraction from furan synthesis: assays 2 (140 °C for 90 min) and 8 (120 °C for 150 min).

at 1637 cm^{-1}, corresponding to C=C stretching vibrations of aromatic structures, indicating partial cleavage of lignin linkages during pretreatment.[57] Finally, vibrations around 1126 cm^{-1} refer to C–O and C–C stretching in cellulose and hemicellulose; the increased intensity in this region suggests greater exposure and accessibility of cellulose, favoring subsequent sugar-conversion reactions.[29]

For the samples obtained after HMF and FF synthesis (assays 2 and 8), an intense band was observed in the region of 1735 cm^{-1}, associated with C=O stretching of ester, aldehyde, and carboxylic acid groups. This band is characteristic of oxygenated compounds derived from carbohydrate dehydration, such as HMF and FF, typical products of sugar conversion in acidic media.[61,62] In assay 8, the band around 1374 cm^{-1} was attributed to C–H deformation in methyl and methylene groups, commonly associated with substituted furan structures. The bands between 1228 and 1042 cm^{-1} correspond to C–O–C and C–O stretching of alcohols, ethers, and oxygenated heterocyclic compounds.[37,38] These spectral changes confirm the formation of furanic products and highlight the catalytic efficiency of the ChCl:OA DES system in converting carbohydrates into high value-added compounds.

Crystallinity

Samples of raw cupuaçu peel and the solid fraction after pretreatment with DES using US and ATC were subjected to XRD analysis to investigate the crystallinity behavior (Figure 6).

The CrI in raw cupuaçu peel was 54.14%, a value close to that reported by Marasca *et al.*,[63] who found 54.3% crystallinity in fresh cupuaçu peel. The CrI values of samples pretreated with different DES combined with different methods ranged from 50.8 to 57.56% for the

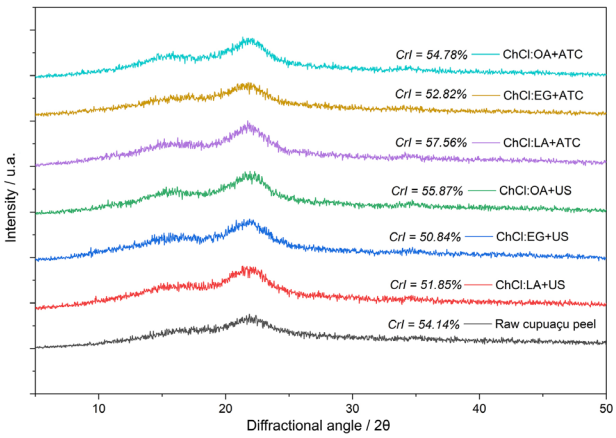

Figure 6. XRD diffractograms of raw cupuaçu peel and of the solid fraction of samples after pretreatment with different DES combined with ultrasound (US) or autoclave (ATC).

ChCl:EG + US and ChCl:LA + ATC systems, respectively. Most of the pretreated samples showed significantly different crystallinity compared to the raw bark. In the pretreatments with ChCl:EG + US and ChCl:LA + US, the crystallinity decreased significantly. This decrease suggests that ultrasonic cavitation, in synergy with the deep eutectic solvent, favored the disorganization of the fibers, as well as the partial removal of amorphous components and peripheral crystalline fractions.[64]

In contrast, most ATC treatments showed slightly higher or preserved crystallinity values, possibly due to the preferential removal of hemicellulose and amorphous lignin, resulting in relative enrichment of the crystalline cellulose fraction. In general, DES promote a reduction in crystallinity, associated with the rupture of hydrogen bonds and the induction of topochemical and morphological changes in the lignocellulosic cell wall. These structural modifications favor the disorganization of crystalline regions, increasing biomass accessibility and enhancing subsequent conversion steps.[65, 66]

Pretreatments with ChCl:LA + ATC and ChCl:OA + US promoted the greatest increase in crystallinity index compared to the raw biomass (CrI = 54.14%), indicating preferential removal of amorphous fractions, especially hemicellulose and lignin. In contrast, the ChCl:LA + US, ChCl:EG + US, and ChCl:EG + ATC treatments resulted in slight reductions in crystallinity, possibly due to greater disorganization of the cellulosic structure.[67]

Figure 7 shows SEM images of raw cupuaçu peel and peel pretreated with different DES using ultrasound and autoclave.

A well-ordered and relatively smooth structure, with limited damage to the cell wall, was observed for raw cupuaçu peel (Figure 7a). After DES pretreatments using both methods (ultrasound and autoclave), a gradual exposure of the physical structure of the biomass was observed, accompanied by pronounced morphological damage (Figures 7b-7g). This transition from a smooth and compact surface (Figure 7a) to a more fibrillated and porous structure (Figures 7b-7g) is associated with partial removal of amorphous polymers, mainly lignin and hemicellulose, which act as binding agents between cellulose microfibrils. According to the literature,[68] this behavior confirms that DES promote partial delignification and increase the enzymatic and reactive accessibility of biomass.

The nature of the DES HBD significantly influences the efficiency of β–O–4 lignin bond cleavage, enhancing lignin removal and leading to more pronounced surface erosion of the biomass.[69] Systems with acidic HBDs combined with hydrothermal equipment exhibit greater delignification and more intense morphological alterations. This behavior explains the greater structural opening and fragmentation observed mainly in the micrographs of sample (Figure 7g), which was pretreated with an acidic DES formulation combined with the use of an autoclave, such as ChCl:OA + ATC.[70] According to Sánchez-Badillo *et al.*,[71] the Kamlet-Taft acidity parameters (α, β) of DES control the extent of protonation of cellulose –OH groups; DES with higher acidity (α) increase interaction with hydroxyl groups, facilitating the weakening of O–H···O hydrogen bonds and swelling of the microfibrils.

Thermal stability and decomposition behavior

Thermal stability was evaluated by TGA at a heating rate of 10 °C min^{-1} up to 900 °C (Table 4).

The untreated cupuaçu peel exhibited a main degradation temperature (T_d) at 331 °C with a mass loss of 69% and a minor volatile fraction (3%). In contrast, all DES-treated samples showed significantly higher T_d values (361-371 °C), corresponding to an increase of 30-40 °C relative to the raw biomass, indicating enhanced thermal stability. Such a shift toward higher degradation temperatures suggests structural modification of the lignocellulosic matrix, likely involving partial removal of hemicellulose and enrichment in more thermally resistant fractions. According to Yang *et al.*,[72] hemicellulose decomposes between 220-315 °C, cellulose between 315-400 °C, and lignin over a broad range of 160-900 °C. The increase in T_d to ca. 370 °C indicates that the dominant degradation event in DES-treated samples is associated primarily with cellulose and more condensed aromatic domains rather than hemicellulose. The volatile content remained low in all treated materials (≤ 1-6%), consistent with reduced extractives and improved structural consolidation. Lower volatile fractions are commonly

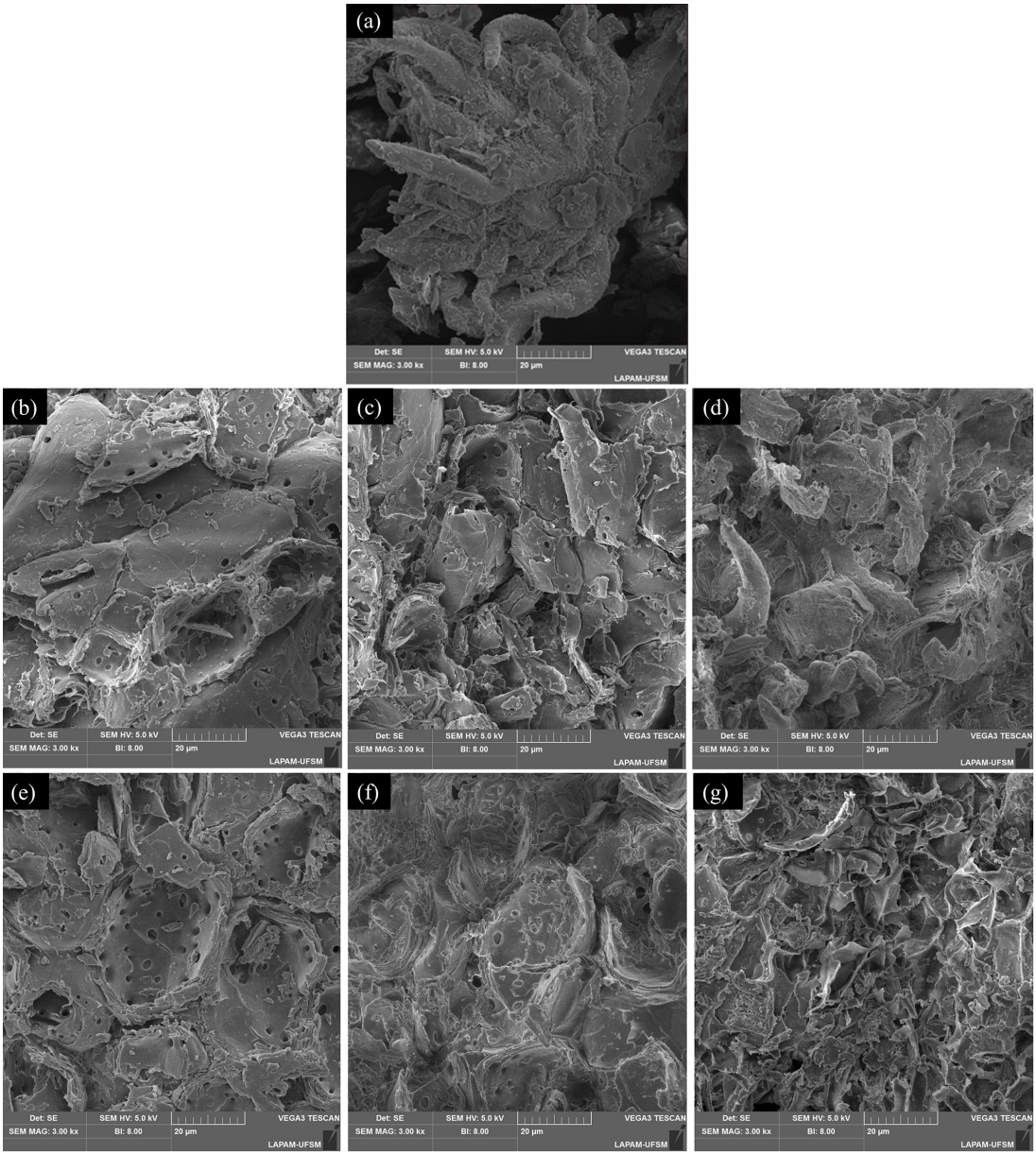

Figure 7. SEM images. (a) raw cupuaçu peel, (b) samples pretreated with ChCl:LA + US, (c) ChCl:EG + US, (d) ChCl:OA + US, (e) ChCl:LA + ATC, (f) ChCl:EG + ATC, (g) ChCl:OA + ATC.

Table 4. Thermogravimetric data of from raw cupuaçu peel and samples pre-treated with different DES combined with ultrasound (US) or autoclave (ATC)

Sample	Volatile / °C	Mass loss / %	T_d	Mass loss / %
ChCl:OA + US	25	≤ 1	371	81
ChCl:EG + US	34	6	369	80
ChCL:LA + US [a]	44	6	365	76
ChCl:OA + ATC[b]	49	4	361	76
ChCl:EG + ATC	35	5	368	62
ChCl:LA + ATC	34	≤ 1	375	86
Raw cupuaçu peel[c]	23	2	331	69

[a]The sample exhibited a additional thermal decomposition step at 298 °C, with mass losses of 25%; [b]two additional decomposition steps were observed at 134 and 252 °C, with mass losses of 5 and 13%, respectively; [c]the sample exhibited a additional thermal decomposition step at 205 °C, with mass losses of 5%. T_d: degradation temperature; ChCl: choline chloride; LA: lactic acid; EG: ethylene glycol; OA: oxalic acid; US: ultrasound; ATC: autoclave.

correlated with higher fixed-carbon content and increased aromatic condensation in lignocellulosic systems.[73]

This behavior suggests that DES treatment promotes partial reorganization of the biomass structure, resulting in materials with greater thermal robustness. Quantitatively, mass loss during the main degradation stage ranged from 62 (ChCl:EG + ATC) to 86% (ChCl:LA + ATC). The lower value observed for ChCl:EG + ATC may indicate a higher residual carbon fraction or greater structural stabilization. Conversely, the higher mass loss in ChCl:LA + ATC suggests more extensive removal of thermally labile fractions. Such variability reflects the influence of DES composition and treatment conditions on the balance between polysaccharide removal and lignin enrichment. Additional degradation steps observed for ChCl:LA + US (298 °C, 25%) and ChCl:OA + ATC (134 °C, 5%; 252 °C, 13%) indicate multi-stage thermal behavior. Events below 150 °C are typically attributed to bound water and low-molecular-weight compounds, whereas those between 200-300 °C correspond predominantly to hemicellulosic degradation.[74] Chemical modifications of lignocellulosic matrices are known to generate such staged decomposition profiles due to altered intermolecular interactions and redistribution of structural components.[75] Overall, the DES-treated cupuaçu peel exhibits enhanced thermal stability, modified devolatilization pathways, and compositional redistribution consistent with selective hemicellulose removal and relative lignin enrichment. These changes corroborate the hypothesis that DES treatment induces structural reorganization in the lignocellulosic network, resulting in materials with greater resistance to thermal degradation, as observed in the Supplementary Information.

Carbohydrate contents

Figure 8 shows the glucose and xylose yields in hydrolysates from raw cupuaçu peel and from samples pretreated with different DES using distinct methodologies.

Glucose contents ranged from 4.25 ± 0.75 to 14.79 ± 0.13 g L^{-1} for the ChCl:EG + ATC and ChCl:OA + ATC pretreatments, respectively. The ChCl:EG + US, ChCl:OA + US, ChCl:LA + ATC, and ChCl:OA + ATC pretreatments resulted in glucose yields higher than the 7.47 ± 0.63 g L^{-1} obtained from raw cupuaçu peel (Figure 8). The values obtained in this study were higher than those reported by Rahman *et al.*,[76] who achieved 3.4 g L^{-1} of glucose from cocoa pod husk (*Theobroma cacao*) by acid hydrolysis under microwave irradiation at 180 °C. Compared with the literature, the ChCl:OA DES system, regardless of the method employed, produced significantly higher yields, exceeding the 9.90 g L^{-1} of glucose reported by Marasca *et al.*,[63] using cupuaçu peel subjected to ultrasound-assisted acidic pretreatment followed by dilute acid hydrolysis. The stable eutectic structure of ChCl:OA DES provides a highly polar and homogeneous medium, favoring biomass solubilization and improving mass and heat transfer during the reaction, thus facilitating carbohydrate extraction.[62,77]

Xylose yields in hydrolysates after pretreatment ranged from 1.49 ± 0.11 to 4.88 ± 0.22 g L^{-1} for the ChCl:OA + ATC and ChCl:LA + ATC systems, respectively. Pretreatments with ChCl:LA + US, ChCl:EG + US, and ChCl:LA + ATC resulted in xylose contents similar to that of raw cupuaçu peel, which yielded 5.04 ± 0.63 g L^{-1}. All values obtained in this study were higher than those reported in the literature[78] for cassava peel, where a xylose concentration of 0.27 g L^{-1} was observed using a similar methodology. Likewise, Rahman *et al.*[76] reported 0.94 g L^{-1} of xylose from cocoa pod husk using microwave-assisted acid hydrolysis. These results reinforce the importance of DES in lignocellulosic biomass pretreatment, as they directly contribute to lignin degradation and facilitate the conversion of cellulose and hemicellulose into monosaccharides.[29,58]

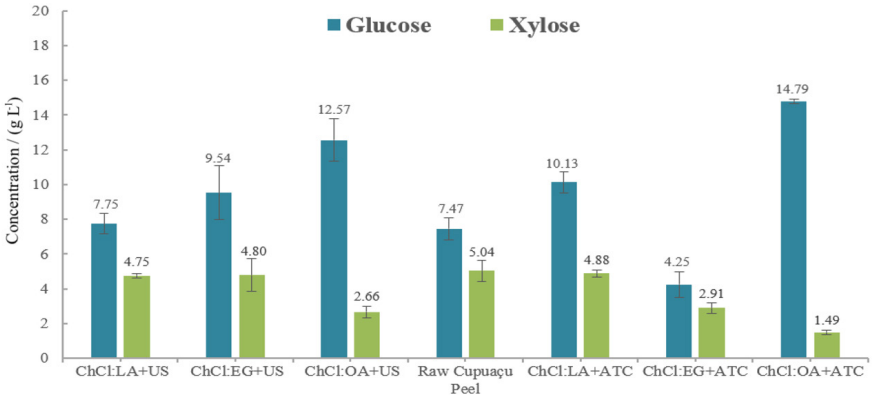

Figure 8. Glucose and xylose yields obtained from hydrolysates of raw cupuaçu peel and samples pretreated with different DES combined with ultrasound (US) or autoclave (ATC).

Table 5. Analysis of variance (ANOVA) for main effects and interaction between methods (ultrasound and autoclave) and DES types (ChCl:LA, ChCl:EG, ChCl:OA), as well as the control (raw cupuaçu peel), on glucose and xylose yields

Sources of variation	GL	QM		*p*-value	
		Glucose / (g L^{-1})	Xylose / (g L^{-1})	Glucose	Xylose
Methods	1	0.2312[ns]	4.2924[a]	0.5845	0.0002
Types of DES	2	72.7717[a]	11.5771[a]	0.0001	0.0001
Methods *vs.* types of DES	2	28.7745[a]	1.5621[a]	0.0001	0.0001
Factorial	5	40.6647[a]	6.1141[a]	0.0001	0.0031
Control *vs.* factorial	1	19.1490[a]	8.0610[a]	0.0002	0.0001
Treatments	6	37.0787[a]	6.4386[a]	0.0001	0.0001
Waste	14	0.7381	0.1743	–	–
Total	20	57.7803	41.0733	–	–

[a]Significant at $p < 0.05$. GL: degrees of freedom; QM: mean square; ns: not significant; control: raw cupuacu peel.

Statistical analysis

Table 5 presents the analysis of variance (ANOVA), considering the factors method (ultrasound and autoclave), DES type (ChCl:LA, ChCl:EG, and ChCl:OA), their interaction, and the additional treatment (raw cupuaçu peel).

ANOVA showed that the different DES types and the interaction between factors (methods × DES type) significantly affected ($p < 0.05$) glucose yield. This indicates that both the DES type and its combination with the pretreatment method were decisive for the observed glucose levels (Table 5). In contrast, the isolated effect of method was not statistically significant, reinforcing that process efficiency is directly conditioned by its interaction with the solvent type employed.

For xylose, ANOVA results indicated that both the pretreatment method and DES type had significant effects ($p < 0.05$), showing that the release of this carbohydrate is simultaneously influenced by operational conditions and the nature of the green solvent. The interaction between factors (methods × DES types) was also statistically significant, indicating the need to unfold the interactions (methods × DES types and DES types × methods) for a more detailed understanding of the combined effects. Overall, comparison between the factorial design and the control revealed significantly higher glucose and lower xylose levels, confirming that DES pretreatments were efficient and selective for sugar release from cupuaçu peel.

Carbohydrate results were subjected to statistical tests, which showed significant differences in glucose and xylose yields as a function of DES type and of the ultrasound and autoclave methods used in the study (Table 6).

For glucose, the ChCl:OA + ATC DES produced the highest yield (14.79 g L^{-1}), differing significantly from the other treatments and being 97.90% higher than the control, indicating greater efficiency in lignocellulose deconstruction and carbohydrate release. The use of acidic DES can significantly enhance carbohydrate release, and these authors reported a glucose yield of 79.7% from rice straw treated with the DES ChCl:formic acid.[62] The ultrasound method combined with ChCl:OA also showed a high yield (12.56 g L^{-1}), corresponding to a 69.72% increase relative to raw cupuaçu peel. Pretreatment with ChCl:OA promotes structural changes on the substrate surface, enlarging pores and increasing cellulose accessibility, resulting in higher glucose yields.[79,80]

Table 6. Mean glucose and xylose yields for raw cupuaçu peel (control) and for samples pretreated with DES (ChCl:LA, ChCl:EG, and ChCl:OA) combined with ultrasound or autoclave

Methods evaluated	Glucose yield / (g L^{-1})			Xylose yield / (g L^{-1})		
	DES type			DES type		
	ChCl:LA	ChCl:EG	ChCl:OA	ChCl:LA	ChCl:EG	ChCl:OA
Ultrasound method	7.75bC[ns]	9.53aB[a]	12.56bA[a]	4.75aA[ns]	4.79aA[ns]	2.66aB[a]
Autoclave method	10.12aB[a]	4.5bC[a]	14.79aA[a]	4.88aA[ns]	2.91bB[a]	1.49bC[a]
Control		7.47			5.04	

For the same DES, means followed by the same lowercase letter in a column do not differ by the Scott-Knott test ($p < 0.05$). For different DES types within the same method, means followed by the same uppercase letter in a row do not differ by the Scott-Knott test ($p < 0.05$). ns and a: not significant and significant ($p < 0.05$), respectively, for comparison of treatments with the control by the test of Dunnett. ChCl: choline chloride; LA: lactic acid; EG: ethylene glycol; OA: oxalic acid.

Acid pretreatments using DES have stood out for their selective ability to promote the disruption of the lignocellulosic matrix, resulting in greater glucose release compared to xylose. This selectivity may be directly associated with the catalytic acid action on the β-1,4 glycosidic bonds of cellulose during hydrolysis, considering that hemicellulose chains tend to be partially solubilized in the initial stages of the pretreatment.[81,29] DES formed with organic acids such as oxalic and lactic acids have low pK_a and proton-donating capacity, acting as mild acid catalysts.[82] This property facilitates partial hydrolysis of crystalline cellulose, enhancing lignocellulosic biomass accessibility and consequently promoting greater glucose release during subsequent hydrolysis.[83] In addition, protons released by acidic DES contribute to the cleavage of ester and ether linkages between lignin and carbohydrates, reducing the recalcitrance of the cell wall.[56]

With respect to xylose, the ChCl:EG + ATC, ChCl:LA + US and ATC, and ChCl:OA + US pretreatments did not differ significantly from raw cupuaçu peel, according to the Scott-Knott test combined with the test of Dunnett ($p < 0.05$). In contrast, the ChCl:EG + US and ChCl:OA + US and ATC treatments produced xylose contents lower than those of raw peel, indicating process selectivity toward the hemicellulosic fraction. DES effectiveness depends directly on their formulation and operating conditions and does not necessarily guarantee xylose extraction, since some DES may have greater affinity for other sugars, such as glucose.[62,76]

According to the literature,[84] acidic DES enhance selective hydrolysis, facilitating the release of sugars and phenolic compounds, and may promote the formation of furan derivatives from xylose. The acidity of these solvents is a key determinant of extraction selectivity, intensifying polysaccharide hydrolysis because organic acids promote hemicellulose bond cleavage and contribute to furan formation, whereas glucose release occurs in a more controlled manner from cellulose.[85] Thus, the behavior of acidic DES explains the greater selectivity observed in this study for glucose production, as cellulose, even when only partially hydrolyzed, provides monosaccharides in a more stable and gradual way. Nonetheless, DES-based pretreatment of lignocellulosic biomass stands out as a viable and environmentally sustainable alternative for increasing carbohydrate conversion efficiency and improving the valorization of this feedstock in biorefineries.[86]

Synthesis of furanic compounds

Figure 9 shows HMF and FF yields obtained from synthesis using the hydrolysate pretreated with ChCl:OA + ATC, which was the system that provided the highest glucose yield. The values result from experimental optimization conducted using a FCD, as described in Table 1.

HMF yields ranged from 0.78% in assay 2 (140 °C for 90 min) to 1.46% in assay 8 (120 °C for 150 min) (Figure 9). These results are comparable to those reported by Scapin *et al.*,[38] which varied between 0.91% (100 ºC for 60 min) and 3.03% (120 ºC for 120 min) of HMF from 2.5 mL hydrolyzed pequi peel, using 1 g of [BMIM][Br] ionic liquid under similar conditions. In a study conducted by Huynh *et al.*,[30] a DES + DMSO system combined with $AlCl_3{\cdot}6H_2O$ as catalyst at 150 °C for 120 min resulted in HMF yields of 18.49 and 19.86% from corn stalk and rice straw, respectively.

The use of choline chloride-oxalic acid DES (ChCl:OA) has proven highly effective for HMF synthesis due to its ability to promote selective and efficient glucose dehydration. The moderate acidity of oxalic acid acts as a protic catalyst, accelerating conversion reactions without causing excessive sugar degradation.[61] Temperature is a critical factor in HMF synthesis using DES containing oxalic acid as HBD. Thi Ngo *et al.*,[87] reported that the highest HMF yield (29%) was obtained at 100 °C, whereas

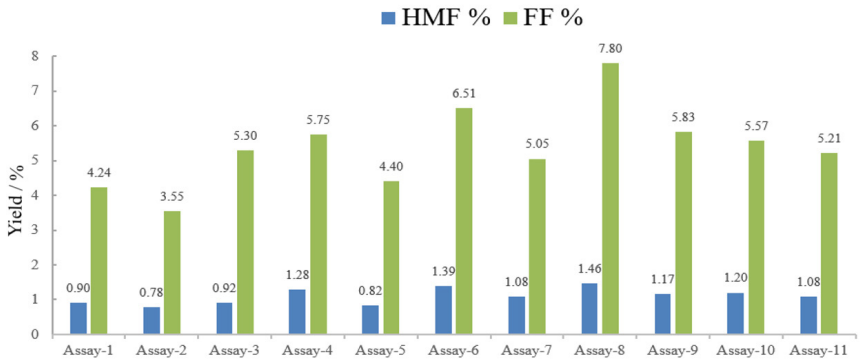

Figure 9. Yields of furanic compounds obtained in synthesis using hydrolysate from cupuaçu peel pretreated with oxalic acid-based DES combined with autoclave. Assay 1: 100 °C for 90 min; assay 2: 140 °C for 90 min; assay 3: 100 °C for 150 min; assay 4: 140 °C for 150 min; assay 5: 100 °C for 120 min; assay 6: 140 °C for 120 min; assay 7: 120 °C for 90 min; assay 8: 120 °C for 150 min; assays 9-11: 120 °C for 120 min.

at room temperature productivity was below 5%. This result demonstrates that increasing temperature favors the glucose dehydration rate, promoting more efficient and selective conversion to HMF. Thus, ChCl:OA DES stands out as a promising solvent, combining catalytic activity, conversion efficiency, and sustainability in HMF production from renewable sources such as lignocellulosic biomass.

FF yields ranged from 3.55 to 7.80%, with emphasis on assays 2 (140 °C for 90 min) and 8 (120 °C for 150 min), respectively. These results are consistent with those reported by Bizzi *et al.*,[88] who obtained FF yields of 3.64% for rice husk, 4.99% for sugarcane straw, and 7.24% for grass, all under ultrasound-assisted hydrolysis. According to To *et al.*,[61] DES have high potential for carbohydrate conversion into furanic compounds, demonstrating their applicability in the synthesis of platform chemicals from biomass. This efficiency may be related to solvent solubility and polarity, which favor reagent interaction and reaction kinetics, resulting in higher furanic compound yields.[30] Guo and Qi *et al.*,[82] emphasized that acidic DES with low pKa act as mild catalysts, promoting selective reactions for HMF or FF formation, highlighting their moderate acidity compared with traditional mineral acids.

Response surface analysis

Figure 10 shows the response surface plots obtained from the experimental design for optimization of HMF and FF synthesis. It can be observed that, in the system studied, the combination of temperature and reaction time that resulted in the maximum yields for the HMF and FF biocompounds was 120 °C for 150 min.

The analysis ANOVA (Table 7) of the quadratic model applied to response surface design, considering a significance level of $\alpha = 0.05$, showed significance for HMF yields, indicating a correlation between temperature and reaction time. For FF yield, the model did not show statistical significance; however, variations associated with reaction time were observed. The mathematical model showed moderate statistical support, with coefficients of determination (R^2) of 76.73% for HMF and 70.17% for FF. These results indicate that the quadratic adjustment was used for exploratory purposes, aiming to identify possible non-linear trends among the evaluated variables.

The model equation was obtained using temperature (x_1) and reaction time (x_2) as variables. Equations 7 and 8 were established for coded variables, where Y_1 represents HMF yield and Y_2 represents FF yield:

$$Y_1 = 1.20 + 0.13x_1 - 0.18x_1^2 + 0.15x_2 + 0.12x_1x_2 \quad (7)$$

$$Y_2 = 5.89 + 0.31x_1 - 0.93x_1^2 + 1x_2 + 0.29x_1x_2 \quad (8)$$

ANOVA indicated no significant effects of temperature (x_1) or the interaction between temperature and time (x_1x_2) on HMF synthesis; however, reaction

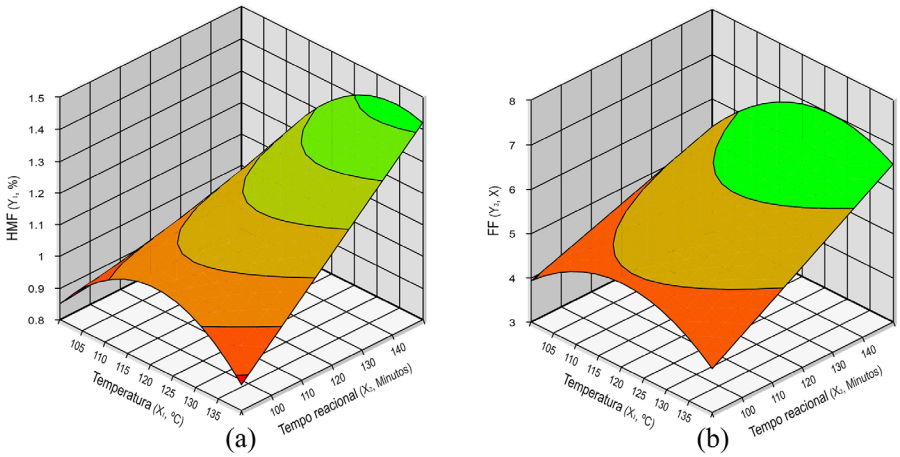

Figure 10. Response surface plots for the synthesis of (a) HMF and (b) FF.

Table 7. ANOVA parameters for the quadratic model of the response surface design for HMF and FF

Sources variation	Sum of squares		Degrees of freedom		Mean square		*p*-Value	
	HMF	FF	HMF	FF	HMF	FF	HMF	FF
Regression	0.4	9.3	4	4	0.1	2.3	0.04342	0.08246
Residual	0.1	4.0	6	6	0.0	0.7	–	–
Total	0.5	13.3	10	10	–	–	–	–

HMF: 5-hydroxymethylfurfural; FF: furfural; *p*-value at 5% significance level.

time (x_2) showed a statistically significant effect, indicating that within the evaluated range this factor significantly influenced the HMF yield. A similar behavior was observed for FF production, as the full factorial design (FCD) revealed a significant effect only for reaction time (x_2), while temperature (x_1) and the interaction term (x_1x_2) were not statistically significant, as observed in the pareto chart in Figure 11.

Conclusions

The composition of cupuaçu peel indicated favorable cellulose and hemicellulose contents, supporting its use as a sustainable source of bioproducts. Significant structural alterations, evidenced by FTIR, XRD, SEM, and TGA, confirm the efficiency of the pretreatments applied to cupuaçu peel. Most of the pretreated samples showed alterations in crystallinity compared to the raw biomass. Associated with the disorganization of the lignocellulosic matrix observed in the tests, this behavior indicates a greater susceptibility of the biomass to chemical attack, reinforcing the potential for valorization of this Amazonian residue.

The use of DES in pretreatment, combined with ultrasound and autoclave methods applied to cupuaçu peel, led to a statistically significant increase in glucose production. The ChCl:OA + ATC and ChCl:OA + US combinations resulted in increases of 97.90 and 69.72%, respectively, relative to untreated biomass. However, xylose yields in the pretreated samples were lower than those observed in the untreated biomass. Statistical analysis elucidated the selective interactions between DES and pretreatment methods, highlighting the effectiveness of the system in deconstructing lignocellulosic materials.

Optimization of reaction conditions for HMF and FF production resulted in maximum yields of 1.46 and 7.80%, respectively. This underscores the effectiveness of the biotechnological approach used to synthesize biobased compounds from hydrolysate of DES-pretreated cupuaçu peel. Response surface analysis identified optimal conditions of 120 °C for 150 min for HMF and FF, confirming the potential of DES for converting cupuaçu peel into platform biocompounds.

The results confirm that DES constitute a versatile and efficient reaction medium for the fractionation and valorization of cupuaçu peel. The selective synthesis of HMF and FF highlights the potential of the methodology as a promising alternative to conventional pretreatments, contributing to the development of integrated processes aimed at the valorization of agro-industrial waste in a circular biorefinery context.

Supplementary Information

Supplementary information is available free of charge at http://jbcs.sbq.org.br as PDF file.

Data Availability Statement

The data supporting the results reported in this article are available from the corresponding author upon reasonable request. The datasets include raw experimental data, chromatographic analyses (HPLC), Fourier-transform infrared spectroscopy (FTIR) spectra, X-ray diffraction (XRD) data, and other materials generated and analyzed during the course of this study.

Acknowledgments

The authors would like to express their gratitude to the Federal University of Tocantins (UFT) for the support received. This publication was funded by the UFT's Pro-Rectorate for Research (PROPESQ), through call for proposals No. 019/2023 and No. 145/2025, and by the PPGCiamb Graduate Program, through call for proposals No. 21/2023.

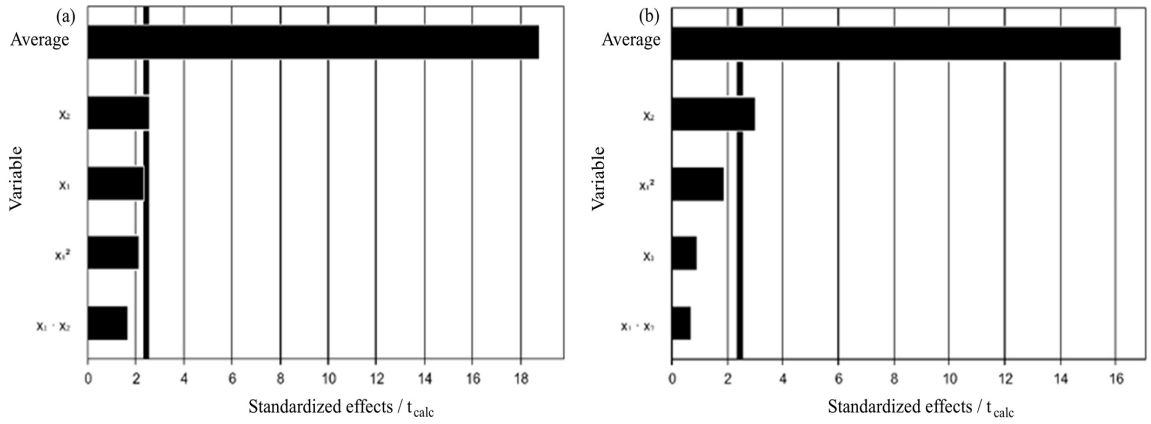

Figure 11. Pareto chart of standardized effects for (a) HMF and (b) FF, where x_1 is temperature and x_2 is reaction time.

Author Contributions

D. M. C.: conceptualization, data curation, formal analysis, funding acquisition, investigation, visualization, and writing (original draft, review, and editing); J. R. S.: data curation, visualization, and writing of the original draft; A. A. R.: data curation, formal analysis, visualization, and composition of figures; J. M. P.: formal data analysis, data curation, application of statistical analysis software, and writing of the original draft; D. A. B.: formal analysis, data curation, validation, visualization, and software; G. G. P.: data formal analysis, data curation and software; C. P. F.: data formal analysis, data curation, software, validation, writing original draft; E. S.: data curation, formal analysis, funding acquisition, project administration and resources, visualization, and writing (review and editing).

References

1. Chen, J.; Ma, X.; Liang, M.; Guo, Z.; Cai, Y.; Zhu, C.; Wang, Z.; Wang, S.; Xu, J.; Ying, H.; *Waste* **2024**, *2*, 451. [Crossref]
2. Bajpai, P.; *Microorganisms and Enzymes for Lignocellulosic Biorefineries*; Elsevier: Amsterdam, 2024.
3. Amesho, K. T. T.; Chen, S.-C.; Wu, T.-Y.; Ponnusamy, V. K.; Lin, Y.-C.; *Environ. Technol. Innov.* **2023**, *29*, 102982. [Crossref]
4. Wang, Y.; Liu, J.-Y.; Sun, J.; Shangdiar, S.; Amesho, K. T. T.; Lin, Y.-C.; Peng, Y.-P.; Chang, K.-L.; *Environ. Sci. Pollut. Res. Int.* **2021**, *28*, 40715. [Crossref]
5. Tong, J.; Hu, W.; Qin, Y.; Liu, Y.; *Cellulose* **2023**, *30*, 4773. [Crossref]
6. Segers, B.; Nimmegeers, P.; Spiller, M.; Tofani, G.; Jasiukaitytė-Grojzdek, E.; Dace, E.; Kikas, T.; Marchetti, J. M.; Rajić, M.; Yildiz, G.; Billen, P.; *RSC Sustainability* **2024**, *2*, 3730. [Crossref]
7. Martins, J. R.; Schmatz, A. A.; Salazar-Bryan, A. M.; Brienzo, M.; *Sugar Tech* **2022**, *24*, 1540. [Crossref]
8. Xie, S.; Yang, Q.; Wang, Q.; Zhou, H.; Bartocci, P.; Fantozzi, F.; *Energy Convers. Manage.* **2023**, *288*, 117155. [Crossref]
9. Shafique, S.; Belousov, A. S.; Rashid, R.; Shafiq, I.; Aziz, K. H. H.; Riaz, N.; Khan, M. S.; Shaheen, A.; Ishaq, M.; Akhter, P.; Hussain, M.; *J. Mol. Liq.* **2025**, *419*, 126769. [Crossref]
10. Tang, W.; Fan, B.; Wang, X.; Huang, C.; Tang, Z.; He, Y.; *Ind. Crops Prod.* **2023**, *206*, 117587. [Crossref]
11. Sharma, V.; Tsai, M.-L.; Chen, C.-W.; Sun, P.-P.; Patel, A. K.; Singhania, R. R.; Nargotra, P.; Dong, C.-D.; *Bioresour. Technol.* **2022**, *360*, 127631. [Crossref]
12. Ullah, A.; Zhang, Y.; Liu, C.; Qiao, Q.; Shao, Q.; Shi, J.; *Bioresour. Technol.* **2023**, *369*, 128394. [Crossref]
13. Jofre, F. M.; Prado, C. A.; Shibukawa, V. P.; Rodrigues, B. G.; Sarangi, P. K.; Chandel, A. K.; *Int. J. Biol. Macromol.* **2025**, *305*, 140957. [Crossref]
14. Amesho, K. T. T.; Cheng, P.-C.; Chang, K.-L.; Peng, Y.-P.; Jhang, S.-R.; Lin, Y.-C.; *Bioresour. Technol.* **2022**, *363*, 127969. [Crossref]
15. Araujo, N. M. P.; Arruda, H. S.; Marques, D. R. P.; de Oliveira, W. Q.; Pereira, G. A.; Pastore, G. M.; *Food Res. Int.* **2021**, *147*, 110520. [Crossref]
16. Souza, A. G. C.; Alves, R. M.; Lopes Filho, R. P.; *Bancos Genéticos de Cupuaçu*; Embrapa Brasília, 2021. [Link] accessed in June 2026
17. Cardoso, J. E. P.; Nogueira, L. P.; Silva, A. M. G.; Alonso, J. C.; Feliciano, D. E. F.; Monteiro, H. S. A.; Brito, S. N. S.; Cunha Jr., P. H. H.; Redig, M. S. F.; Bronze, A. B. S.; *Desenvolvimento Rural Sustentável: Novas Perspectivas*; Editora Científica Digital, 2024.
18. Borges, M. S.; Santos, J. R.; Pedroza, M. M.; Rambo, M. K. D.; Assumpção, D. B.; Frizzo, C. P.; Burrow, R. A.; Scapin, E.; *J. Braz. Chem. Soc.* **2025**, *36*, e-20240202. [Crossref]
19. Golveia, J. C. S.; Santiago, M. F.; Sales, P. T. F.; Sartoratto, A.; Ponezi, A. N.; Thomaz, D. V.; Gil, E. S.; Bara, M. T. F.; *Prep. Biochem. Biotechnol.* **2018**, *48*, 541. [Crossref]
20. Marasca, N.; Cardoso, I.; Rambo, M.; Bertuol, D.; Guarda, E.; Scapin, E.; *J. Braz. Chem. Soc.* **2022**, *33*, 906. [Crossref]
21. ASTM D3173-03: *Standard Test Method for Determination of Moisture in the Analysis Sample of Coal and Coke*; ASTM International: West Conshohocken, PA, USA, 2003. [Link] accessed in June 2026
22. ASTM D3175-07: *Standard Test Method for Volatile Matter in the Analysis Sample of Coal and Coke*; ASTM International: West Conshohocken, PA, USA, 2007. [Link] accessed in June 2026
23. ASTM D3174-04: *Standard Test Method for Ash in the Analysis Sample of Coal and Coke*; ASTM International: West Conshohocken, PA, USA, 2004. [Link] accessed in June 2026
24. NREL/TP-510-42619: *Determination of Extractives in Biomass*; National Renewable Energy Laboratory: Denver, CO, USA, 2011. [Link] accessed in June 2026
25. Detmann, E.; Silva, L. F. C.; Rocha, G. C.; Palmas, M. N. N.; Rodrigues, J. P. P.; *Métodos para Análise de Alimentos - INCT - Ciência Animal*; Suprema: Visconde do Rio Branco, 2021. [Link] accessed in June 2026
26. Association of Official Analytical Chemists (AOAC); *Official Methods of Analysis*, 15th ed.; AOAC: Arlington, TX, USA, 1990. [Link] accessed in June 2026
27. Ding, T. Y.; Hii, S. L.; Ong, L.; *BioResources* **2012**, *7,* 1540. [Crossref]
28. Rocha, G. J. M.; *Deslignificação de Bagaço de Cana de Açúcar Assistida por Oxigênio*; PhD Thesis, University of São Paulo, Piracicaba, Brazil, 2000. [Link] accessed in June 2026
29. Zhang, L.; Zhang, C.; Ma, Y.; Zhao, X.; Zhang, X.; *Ind. Crops Prod.* **2024**, *211*, 118257. [Crossref]

30. Huynh, Q. T.; Zhong, C.-T.; Huang, Q.; Lin, Y.-C.; Chen, K.-F.; Liao, C.-S.; Dong, C.-D.; Chang, K.-L.; *Bioresour. Technol.* **2023**, *387*, 129590. [Crossref]
31. Pradhan, D.; Jaiswal, S.; Tiwari, B. K.; Jaiswal, A. K.; *Int. J. Biol. Macromol.* **2024**, *281*, 136213. [Crossref]
32. Huang, C.; Cheng, J.; Zhan, Y.; Liu, X.; Wang, J.; Wang, Y.; Yoo, C. G.; Fang, G.; Meng, X.; Ragauskas, A. J.; Song, X.; *Bioresour. Technol.* **2022**, *362*, 127771. [Crossref]
33. Dunning, J. W.; Dallas, D. E.; *Anal. Chem.* **1949**, *21*, 727. [Crossref]
34. Sasmal, S.; Goud, V. V.; Mohanty, K.; *Biomass Bioenergy* **2012**, *45*, 212. [Crossref]
35. Barbosa, J. C.; Maldonado Jr., W.; *AgroEstat: Sistema para Análises Estatísticas de Ensaios Agronômicos*, version 1; FCAV/UNESP: Jaboticabal, SP, Brazil, 2015. [Link] accessed in June 2026
36. Cruz, C. D.; *Acta Sci., Agron.* **2013**, *35*, 271 [Crossref]; Portal GENES. [Link] accessed in June 2026
37. Niakan, M.; Masteri-Farahani, M.; Seidi, F.; *Fuel* **2023**, *337*, 127242. [Crossref]
38. Scapin, E.; Rambo, M. K. D.; Viana, G.; Borges, M.; Rambo, M. C. C.; Carneiro, C.; *J. Braz. Chem. Soc.* **2020**, *31*, 1383. [Crossref]
39. Rodrigues, M. I.; Costa, P.; *Protimiza Experimental Design,* version 1; Protimiza: Campinas, Brazil, 2014. [Link] accessed in June 2026
40. Cai, C.; Liu, Q.; Tan, J.; Wang, T.; Zhang, Q.; Ma, L.; *BioResources* **2017**, *12*, 1201. [Crossref]
41. Suárez-Patlán, E. E.; Espinosa-Solares, T.; Herbert-Pucheta, J. E.; Hernández-Núñez, E.; Zuleta-Prada, H.; *Chap. Ser. Cienc. For. Ambient.* **2024**, *30*, 35. [Crossref]
42. Silva, G. M.; Moreira, R. J. A.; Cândido, J. E.; da Silva, I. R.; Morais, B. A.; Gouveia, M. J.; Leite, T. C. C.; Sena, A. R.; *Extensão Rural: Práticas e Pesquisas Para o Fortalecimento da Agricultura Familiar*, Vol. 1; Editora Científica Digital: Guarujá, Brazil, 2021.
43. Santana Jr., C. C.; Brito, M. R.; Barbosa, L. N.; Jaconi, A.; Rambo, M. K. D.; Rambo, M. C. D.; *Int. J. Adv. Eng. Res. Sci.* **2020**, *7*, 324. [Crossref]
44. Estacio, J. S. R.; Hoyos, S. A. C.; *Rev. Cient. Dékamu Agropec.* **2022**, *3*, 94. [Crossref]
45. Vieira, T. A. S.; Trugilho, P. F.; Carabineiro, S. A. C.; Zanuncio, A. J. V.; Carvalho, A. G.; Branco-Vieira, M.; *Forests* **2023**, *14*, 2240. [Crossref]
46. Hu, M.; Yuan, L.; Cai, Z.; Zhang, W.; Fu, Q.; Ji, D.; *Bioresour. Technol.* **2023**, *367*, 128242. [Crossref]
47. Sari, I. P.; Octaviani, E. A.; Khansa, S. D.; Fadillah, G.; *Anal. Environ. Chem.* **2024**, *11*, 2540. [Crossref]
48. Bao, Y.; Wang, Y.; Yan, C.; Xue, Z.; *Green Chem. Eng.* **2025**, *6*, 21. [Crossref]
49. Reyes-Obando, A.; Rodríguez-Gutiérrez, R.; Ramírez-González, P. E.; *Mol. Simul.* **2025**, *51*, 1. [Crossref]
50. Chenthamara, B.; Mudedla, S. K.; Subramanian, V.; Gardas, R. L.; *J. Phys. Chem. B* **2025**, *129*, 8448. [Crossref]
51. Lee, C. W.; Lee, K. S.; Ryu, J.-Y.; Choi, K.-H.; *Polpu, Chongi Gisul* **2024**, *56*, 38. [Crossref]
52. Zhang, M.; Zhang, X.; Liu, Y.; Wu, K.; Zhu, Y.; Lu, H.; Liang, B.; *Environ. Sci. Pollut. Res. Int.* **2021**, *28*, 35537. [Crossref]
53. Ahmed, B.; Gwon, J.; Thapaliya, M.; Adhikari, A.; Ren, S.; Wu, Q.; *Cellulose* **2023**, *30*, 2895. [Crossref]
54. Mankar, A. R.; Pandey, A.; Modak, A.; Pant, K. K.; *Renewable Energy* **2021**, *177*, 643. [Crossref]
55. Shukla, A.; Ramteke, S.; Sahu, B. L.; Deb, M. K.; *J. Ravishankar Univ.* **2024**, *37*, 39. [Crossref]
56. Makarem, M.; Lee, C. M.; Kafle, K.; Huang, S.; Chae, I.; Yang, H.; Kubicki, J. D.; Kim, S. H.; *Cellulose* **2019**, *26*, 35. [Crossref]
57. Roslan, M. F.; Luthfi, A. A. I.; Salleh, M. Z. M.; Manaf, S. F. A.; Nasoha, N. Z.; Hariz, H. B.; Tan, J. P.; Abdul, P. M.; *Biomass Convers. Biorefin.* **2025**, *15*, 12825. [Crossref]
58. Chen, X.; Liu, Q.; Li, B.; Wang, N.; Liu, C.; Shi, J.; Liu, L.; *Int. J. Biol. Macromol.* **2024**, *259*, 129354. [Crossref]
59. Souza, L. P. D. E.; Dantas, P. V. F.; Guilherme, A. D. E. A.; Santos, E. S. D. O. S.; Fernandes, F. A. N.; Macedo, G. R. D. E. In *Anais do XX Congresso Brasileiro de Engenharia Química*; Editora Edgard Blücher: São Paulo, Brazil, 2015, p. 2895. [Crossref]
60. Li, M.; He, B.; Chen, Y.; Zhao, L.; *ACS Omega* **2021**, *6*, 25162. [Crossref]
61. To, L. N.; Nguyen, T. H.; Nguyen, T. P.; Phan, H. B.; Nguyen, L. H. T.; Doan, T. L. H.; Van Dang, C.; Tran, P. H.; *Catalysts* **2023**, *13*, 1216. [Crossref]
62. Igbojionu, L. I.; Manayil, J. C.; Fernandez-Castane, A.; *Biomass Convers. Biorefin.* **2025**, *15*, 31107. [Link] accessed in June 2026
63. Marasca, N.; Brito, M. R.; Rambo, M. C. D.; Pedrazzi, C.; Scapin, E.; Rambo, M. K. D.; *Food Sci. Technol.* **2022**, *42*, e48421. [Crossref]
64. Pradhan, D.; Jaiswal, S.; Tiwari, B. K.; Jaiswal, A. K.; *Ultrason. Sonochem.* **2024**, *110*, 107048. [Crossref]
65. Li, F.; Liu, Y.; Jia, J.; Yu, H.; *Bioresour. Technol.* **2023**, *380*, 129110. [Crossref]
66. Kamdem, M. M.; Fouegue, A. T.; Lai, N.; *Energies* **2023**, *16*, 3806. [Crossref]
67. Jang, S.-K.; Jeong, H.; Choi, I.-G.; *Sustainability* **2023**, *15*, 5869. [Crossref]
68. Kalhor, P.; Ghandi, K.; *Molecules* **2019**, *24*, 4012. [Crossref]
69. Wu, Y.; Song, R.; Wu, Z.; Huang, W.; Wang, B.; Cui, F.; Liu, Y.; *BioResources* **2025**, *20*, 6887. [Crossref]
70. Zhang, C.-W.; Xia, S.-Q.; Ma, P.-S.; *Bioresour. Technol.* **2016**, *219*, 1. [Crossref]
71. Sánchez-Badillo, J. A.; Gallo, M.; Rutiaga-Quiñones, J. G.; Garza, J.; López-Albarrán, P.; *Cellulose* **2022**, *29*, 6517. [Crossref]

72. Yang, H.; Yan, R.; Chen, H.; Lee, D. H.; Zheng, C.; *Fuel* **2007**, *86*, 1781. [Crossref]
73. Brebu, M.; Vasile, C.; *J. Anal. Appl. Pyrolysis* **2010**, *79*, 17. [Link] accessed in June 2026
74. Varol, E. A.; Mutlu, Ü.; *Energies* **2023**, *16*, 3674. [Crossref]
75. Raveendran, K.; Ganesh, A.; Khilar, K. C. *Fuel* **1996**, *75*, 987. [Crossref]
76. Rahman, S. A.; Meryandini, A.; Juanssilfero, A. B.; Fahrurrozi; *Int. J. Adv. Sci. Eng. Inf. Technol.* **2023**, *13*, 828. [Crossref]
77. Zhao, X.; Tang, W.; Fan, B.; He, Y.-C.; Ma, C.; *Int. J. Biol. Macromol.* **2025**, *303*, 140417. [Crossref]
78. Pereira, T. N.; Aguiar, A. A.; Gerre, E. B.; *J. Biotechnol. Biodiversity* **2020**, *8*, 187. [Crossref]
79. Fu, X.; Qiao, J.; Xu, Z.; Xu, C.; Li, X.; *Ind. Crops Prod.* **2024**, *210*, 118040. [Crossref]
80. Li, X.; Tang, W.; He, Y.-C.; *Ind. Crops Prod.* **2023**, *206*, 117691. [Crossref]
81. Dai, Y.; van Spronsen, J.; Witkamp, G.-J.; Verpoorte, R.; Choi, Y. H.; *Anal. Chim. Acta* **2013**, *766*, 61. [Crossref]
82. Guo, H.; Qi, X.; *Curr. Opin. Green Sustainable Chem.* **2024**, *47*, 100924. [Crossref]
83. Xu, H.; Kong, Y.; Peng, J.; Song, X.; Liu, Y.; Su, Z.; Li, B.; Gao, C.; Tian, W.; *Bioresour. Technol.* **2021**, *319*, 124209. [Crossref]
84. Grigorakis, S.; Makris, D. P.; *Recycling* **2025**, *10*, 178. [Crossref]
85. Al-Akayleh, F.; Ali Agha, A. S. A.; Olaimat, A. R.; Qinna, N. A.; *Polysaccharides* **2025**, *6*, 82. [Crossref]
86. Pereira, E.; Pereira, D. T. V.; Rabelo, S. C.; Ceriani, R.; Costa, A. C.; *J. Environ. Chem. Eng.* **2025**, *13*, 115303. [Crossref]
87. Thi Ngo, D. K.; Nguyen, T. H.; Nguyen, P. N.; Nguyen, H. T.; Thi Huynh, T. N.; Phan, H. B.; Tran, P. H.; *Heliyon* **2023**, *9*, e21274. [Crossref]
88. Bizzi, C. A.; Santos, D.; Sieben, T. C.; Motta, G. V.; Mello, P. A.; Flores, E. M. M.; *Ultrason. Sonochem.* **2019**, *51*, 332. [Crossref]

Submitted: December 8, 2025
Accepted Article online: May 22, 2026
Final version online: June 23, 2026